IEICE TRANS. COMMUN., VOL.E92–B, NO.9 SEPTEMBER 2009

PAPER

Pilot-Assisted Channel Estimation for Orthogonal Multi-Carrier DS-CDMA with Frequency-Domain Equalization

Tomoyuki SHIMA[†a)], **Hiromichi TOMEBA**[†], ***Student Members***, ***and*** **Fumiyuki ADACHI**[†], ***Fellow***

SUMMARY Orthogonal multi-carrier direct sequence code division multiple access (orthogonal MC DS-CDMA) is a combination of time-domain spreading and orthogonal frequency division multiplexing (OFDM). In orthogonal MC DS-CDMA, the frequency diversity gain can be obtained by applying frequency-domain equalization (FDE) based on minimum mean square error (MMSE) criterion to a block of OFDM symbols and can improve the bit error rate (BER) performance in a severe frequency-selective fading channel. FDE requires an accurate estimate of the channel gain. The channel gain can be estimated by removing the pilot modulation in the frequency domain. In this paper, we propose a pilot-assisted channel estimation suitable for orthogonal MC DS-CDMA with FDE and evaluate, by computer simulation, the BER performance in a frequency-selective Rayleigh fading channel.

key words: *orthogonal MC DS-CDMA, frequency-domain equalization, pilot-assisted channel estimation*

1. Introduction

A high speed data transmission of over 100 Mbps is demanded in the next generation mobile communication systems. However, the mobile channel is characterized by frequency-selective fading, and therefore, the bit error rate (BER) performance significantly degrades due to severe inter-symbol interference [1], [2]. To avoid the adverse effect of frequency-selective fading, much attention has been paid to the multi-carrier technique, known as multi-carrier code division multiple access (MC-CDMA) [3], [4]. In MC-CDMA, frequency-domain spreading is combined with orthogonal frequency division multiplexing (OFDM). On the other hand, in direct sequence code division multiple access (DS-CDMA), time-domain spreading is used. A good BER performance can be achieved by using frequency-domain equalization (FDE) based on minimum mean square error (MMSE) criterion, since the frequency diversity gain can be obtained [5].

Another CDMA technique is orthogonal multi-carrier direct sequence code division multiple access (orthogonal MC DS-CDMA) [3] which is a combination of time-domain spreading and OFDM. In orthogonal MC DS-CDMA, DS-CDMA is applied to each OFDM subcarrier to transmit a different data symbol stream. The same user-specific spreading code can be used to all subcarriers. Since one data symbol is transmitted on one subcarrier, orthogonal MC DS-CDMA cannot obtain the frequency diversity gain [3], [4], [6]. Recently, we proposed a new orthogonal MC DS-CDMA which can obtain the frequency diversity gain through the use of FDE and provides a good BER performance [7]. Accurate channel estimation is necessary for performing FDE. However, our previous work assumed the ideal channel estimation. In this paper, we propose a pilot-assisted channel estimation suitable for orthogonal MC DS-CDMA with FDE.

The remainder of this paper is organized as follows. Section 2 introduces orthogonal MC DS-CDMA with FDE. In Sect. 3, a proposed pilot-assisted channel estimation is described. Section 4 presents the simulation results for the achievable BER performance in a frequency-selective Rayleigh fading channel. Section 5 offers some conclusions.

2. Orthogonal MC DS-CDMA with FDE

2.1 Overall Transmission System Model

The transmitter/receiver structure of orthogonal MC DS-CDMA with FDE is illustrated in Fig. 1. At the transmitter, a binary data sequence is transformed into a data modulated symbol sequence. The data symbol sequence is serial-to-parallel (S/P) converted to C parallel streams and then each stream is further S/P converted to N_c substreams. All N_c substreams of the cth stream ($c = 0 \sim C-1$) are spread by a user-specific orthogonal spreading code $\{c^c(n);\ n = 0 \sim SF-1\}$. After code-multiplexing C spread substreams, N_c-point inverse fast Fourier transform (IFFT) is applied chip-by-chip to generate the orthogonal MC DS-CDMA signal with N_c subcarriers. As shown in Fig. 2, a sequence of $N_f N_c$ samples (or N_f OFDM symbols) makes a frame. The last N_g samples of a frame are copied as a cyclic prefix (CP) and inserted into the guard interval (GI) to form a frame of $(N_f N_c + N_g)$ samples.

The orthogonal MC DS-CDMA signal is transmitted over a frequency-selective fading channel and is received at a receiver. After the removal of GI, the received signal is decomposed by $N_f N_c$-point fast Fourier transform (FFT) into $N_f N_c$ orthogonal frequency components. After performing FDE, $N_f N_c$-point IFFT is applied to obtain the time-domain signal. This time-domain signal is divided into a sequence of N_c-sample blocks. Then, the orthogonal MC DS-CDMA demodulation is carried out as follows. First, each N_c-sample block is transformed by N_c-point FFT into the frequency-domain signal consisting of N_c subcarrier com-

Manuscript received March 13, 2008.
Manuscript revised February 19, 2009.

[†]The authors are with the Department of Electrical and Communication Engineering, Graduate School of Engineering, Tohoku University, Sendai-shi, 980-8579 Japan.
a) E-mail: shima@mobile.ecei.tohoku.ac.jp

DOI: 10.1587/transcom.E92.B.2874

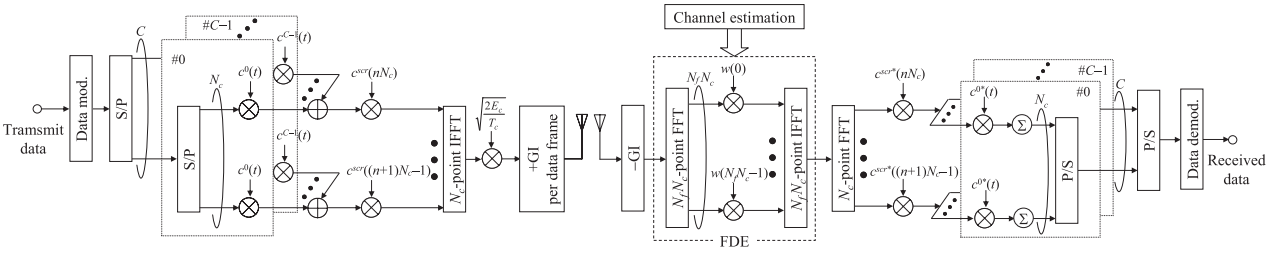

Fig. 1 Transmitter/receiver structure of orthogonal MC DS-CDMA with FDE.

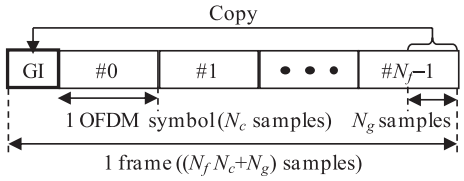

Fig. 2 Frame structure.

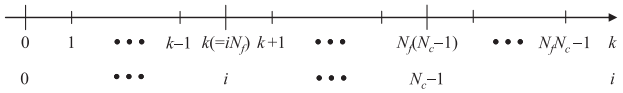

Fig. 3 Relation between subcarrier index i and frequency index k for FDE.

ponents. Then, a sequence of subcarrier components is despread, followed by parallel/serial (P/S) conversion to obtain a sequence of decision variables for data demodulation.

Below, the transmission of one frame is considered. Throughout the paper, sample-spaced discrete-time signal representation is used. Also assumed is the ideal frame synchronization.

2.2 Transmit Signal Representation

The orthogonal MC DS-CDMA signal $s(t)$ to be transmitted in one frame interval can be expressed as

$$s(t) = \sum_{i=0}^{N_c-1} S(i, \lfloor t/N_c \rfloor) \exp\left(j2\pi t \frac{i}{N_c}\right), t = 0 \sim N_f N_c - 1 \tag{1}$$

where $\lfloor x \rfloor$ denotes the largest integer smaller than or equal to x and $S(i,n)$ is the ith subcarrier component given by

$$S(i,n) = \left[\sum_{c=0}^{C-1} d^c(i, \lfloor n/SF \rfloor) c^c(n \bmod SF)\right] c^{scr}(i + nN_c), \tag{2}$$

where $d^c(i,a)$ is the ath data symbol to be transmitted on the ith subcarrier, $c^c(n)$ is the cth orthogonal spreading sequence (belonging to the cth stream) and $c^{scr}(i)$ is the scramble sequence (note that when $N_f < SF$, data symbol to be transmitted on each subcarrier is spread over more-than-one frames). After the power amplification (this is indicated by the multiplication of the factor $\sqrt{2E_c/T_c}$ in Fig. 1) and the insertion of the GI, the orthogonal MC DS-CDMA signal frame is transmitted, where E_c and T_c denote the chip energy and chip period, respectively.

2.3 Received Signal Representation

The fading channel is assumed to have sample-spaced L discrete paths, each subjected to independent block fading. The assumption of block fading means that the path gains stay constant over at least one OFDM symbol duration, and they vary OFDM symbol-by-OFDM symbol. The impulse response $h(\tau)$ of multipath channel can be expressed as

$$h(\tau) = \sum_{l=0}^{L-1} h_l \delta(\tau - \tau_l), \tag{3}$$

where h_l and τ_l are the complex-valued path gain and time delay of the lth path ($l = 0 \sim L-1$), respectively.

The received signal $r(t)$ after removing the GI can be expressed as

$$r(t) = \sqrt{\frac{2E_c}{T_c}} \sum_{l=0}^{L-1} h_l s((t-\tau_l) \bmod N_f N_c) + \eta(t), \quad t = 0 \sim N_f N_c - 1, \tag{4}$$

where $\eta(t)$ is a zero-mean complex Gaussian process with variance $2N_0/T_c$ with N_0 being the single-sided power spectrum density of the additive white Gaussian noise (AWGN).

2.4 FDE

$N_f N_c$-point FFT is applied to decompose $\{r(t);\ t = 0 \sim N_f N_c - 1\}$ into the frequency-domain signal $\{R(k);\ k = 0 \sim N_f N_c - 1\}$. The relation between subcarrier index i and frequency index k is illustrated in Fig. 3. The kth frequency component can be written as

$$\begin{aligned} R(k) &= \sum_{t=0}^{N_f N_c - 1} r(t) \exp\left(-j2\pi k \frac{t}{N_f N_c}\right) \\ &= H(k)S(k) + \Pi(k), \end{aligned} \tag{5}$$

where $S(k)$, $H(k)$ and $\Pi(k)$ are the kth frequency component of the transmitted frame $\{s(t);\ t = 0 \sim N_f N_c - 1\}$, the channel gain, and the noise component due to the AWGN, respectively. They are given by

$$\begin{cases} S(k) = \sum_{t=0}^{N_fN_c-1} s(t)\exp\left(-j2\pi k\frac{t}{N_fN_c}\right) \\ H(k) = \sqrt{\frac{2E_c}{T_c}}\sum_{l=0}^{L-1} h_l\exp\left(-j2\pi k\frac{\tau_l}{N_fN_c}\right) \\ \Pi(k) = \sum_{t=0}^{N_fN_c-1} \eta(t)\exp\left(-j2\pi k\frac{t}{N_fN_c}\right) \end{cases}. \quad (6)$$

FDE is carried out as

$$\hat{R}(k) = w(k)R(k) = H_{eq}(k)S(k) + \Pi_{eq}(k), \quad (7)$$

where

$$\begin{cases} H_{eq}(k) = w(k)H(k) \\ \Pi_{eq}(k) = w(k)\Pi(k) \end{cases}, \quad (8)$$

and $w(k)$ is the MMSE equalization weight, given as

$$w(k) = \frac{H^*(k)}{CN_fN_c|H(k)|^2 + 2\sigma^2}, \quad (9)$$

where σ^2 is the noise power. $H(k)$ and σ^2 need to be estimated [8]. In this paper, we assume the ideal noise power estimation. The estimation of $H(k)$ will be described in Sect. 3.

N_fN_c-point IFFT is applied to obtain the time-domain signal $\{\hat{r}(t);\ t = 0 \sim N_fN_c - 1\}$ as

$$\hat{r}(t) = \frac{1}{N_fN_c}\sum_{k=0}^{N_fN_c-1} \hat{R}(k)\exp\left(j2\pi t\frac{k}{N_fN_c}\right). \quad (10)$$

2.5 Despreading and Data Demodulation

The time-domain signal $\{\hat{r}(t);\ t = 0 \sim N_fN_c - 1\}$ is divided into a sequence of N_c-sample signal blocks. N_c-point FFT is applied to decompose $\{\hat{r}(t);\ t = nN_c \sim (n+1)N_c - 1\}$ into the frequency-domain signal $\{\tilde{R}(i,n);\ i = 0 \sim N_c - 1\}$. The ith subcarrier component $\tilde{R}(i,n)$ can be written as

$$\begin{aligned} \tilde{R}(i,n) &= \frac{1}{N_c}\sum_{t=nN_C}^{(n+1)N_c-1} \hat{r}(t)\exp\left(-j2\pi i\frac{t}{N_c}\right) \\ &= \sqrt{\frac{2E_c}{T_c}}\left(\frac{1}{N_f}\sum_{k=0}^{N_fN_c-1} H_{eq}(k)\Phi^2(i,k)\right)S(i,n) \\ &\quad + \mu_{ISI}(i,n) + \mu_{noise}(i,n), \end{aligned} \quad (11)$$

where the first term is the desired ith subcarrier component, $\mu_{ISI}(i,n)$ is the inter-subcarrier interference (ISI), and $\mu_{noise}(i,n)$ is the noise. $\Phi(i,k)$ is given as

$$\Phi(i,k) = \begin{cases} 1, & \text{if } k = iN_f \\ \frac{1}{N_c}\frac{\sin\left(\pi\frac{k-iN_f}{N_f}\right)}{\sin\left(\pi\frac{k-iN_f}{N_fN_c}\right)}, & \text{otherwise} \end{cases} \quad (12)$$

Despreading is carried out on $\{\tilde{R}(i,n);\ n = aSF \sim (a+1)SF - 1\}$ to obtain the decision variable $\tilde{d}^c(i,a)$ associated with $d^c(i,a)$ as

$$\begin{aligned} \tilde{d}^c(i,a) &= \frac{1}{SF}\sum_{n=aSF}^{(a+1)SF-1} \tilde{R}(i,n)\{c^c(n \bmod SF)c^{scr}(i+nN_c)\}^* \\ &= \sqrt{\frac{2E_c}{T_c}}\left(\frac{1}{N_f}\sum_{k=0}^{N_fN_c-1} H_{eq}(k)\Phi^2(i,k)\right)d^c(i,a) \\ &\quad + \mu_{ISI}(i,a) + \mu_{noise}(i,a) \end{aligned} \quad (13)$$

Note that when $N_f < SF$, despreading is carried out over more-than-one frames. The first term of Eq. (13) represents the data symbol, $\mu_{ISI}(i,a)$ is the residual ISI, and $\mu_{noise}(i,a)$ is the noise.

3. Pilot-Assisted Channel Estimation

$H(k)$ needs to be estimated to compute $w(k)$ of Eq. (9). This paper considers the pilot-assisted channel estimation [9], [10], in which the channel gain $H(k)$ is estimated using the time-multiplexed pilot frame $\{p(t);\ t = 0 \sim N_fN_c - 1\}$. If OFDM with N_fN_c subcarriers is used as the pilot similar to Refs. [9] and [10], the amplitude of frequency component of the pilot frame is the same for all frequencies. However, the peak-to-average power ratio (PAPR) of the pilot frame is N_f times higher than that of the data frame. To make the PAPR of the pilot frame the same as that of data frame, the pilot frame is constructed from N_f OFDM symbols with N_c subcarriers each similar to the data frame. In this paper, three pilot frame designs are considered. The CAZAC sequence [12] is attractive as the pilot sequence since its frequency- and time-domain amplitudes are constant. However, the number of CAZAC sequences is limited (for example, it is less than 128 for the case of 256-bit period) On the other hand, a large number of the pilot sequences exists if PN sequence is used. By using the proposed pilot design (e.g., the repeated pilot), the frequency-domain amplitude of pilot frame can be made constant for all frequencies. In this paper, PN sequences are used as the pilot. The proposed pilot designs are described in detail below.

3.1 Pilot Design

3.1.1 Binary-Pilot

The pilot frame $\{p(t);\ t = 0 \sim N_fN_c - 1\}$ can be expressed as

$$p(t) = \sum_{i=0}^{N_c-1} P(i, \lfloor t/N_c \rfloor)\exp\left(j2\pi t\frac{i}{N_c}\right), \quad (14)$$

where $P(i,n)$ is the ith subcarrier component ($i = 0 \sim (N_c - 1)$) of the nth OFDM symbol ($n = 0 \sim (N_f - 1)$) in the pilot frame. We assume $|P(i,n)| = 1$.

The kth frequency component $R_p(k)$ of the received pilot frame is given by

$$R_p(k) = \sqrt{C\frac{2E_c}{T_c}}H(k)P(k) + \Pi(k),\ k = 0 \sim N_fN_c - 1, \quad (15)$$

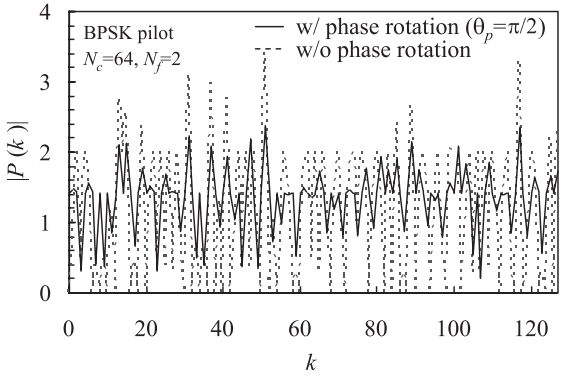

Fig. 4 Frequency response of the pilot frame.

where the pilot power is set to CE_c/T_c to keep it the same as the C-order code-multiplexed data chip power and $P(k)$ is the kth frequency component of the transmitted pilot frame $\{p(t);\ t = 0 \sim N_f N_c - 1\}$, given by

$$P(k) = \sum_{t=0}^{N_f N_c - 1} p(t) \exp\left(-j2\pi k \frac{t}{N_f N_c}\right). \tag{16}$$

$H(k)$ can be estimated using MMSE channel estimation (MMSE-CE) [8]. The channel gain estimate $\hat{H}(k)$ can be obtained as

$$\hat{H}(k) = R_p(k) X^*(k), \tag{17}$$

where $X(k)$ is the reference and is given by [8]

$$X(k) = \frac{P(k)}{|P(k)|^2 + (C/(N_f N_c))^{-1}(E_c/N_0)^{-1}}. \tag{18}$$

For performing MMSE-CE, $X(k)$ requires the knowledge of the received signal power and the noise power. In this paper, we assume the ideal estimation of them.

$\{\hat{H}(k);\ k = 0 \sim N_f N_c - 1\}$ is transformed by applying $N_f N_c$-point IFFT into the instantaneous channel impulse response $\{\hat{h}(\tau);\ \tau = 0 \sim N_f N_c - 1\}$. $\hat{h}(\tau)$ can be obtained as

$$\hat{h}(\tau) = \frac{1}{N_f N_c} \sum_{t=0}^{N_f N_c - 1} \hat{H}(k) \exp\left(j2\pi\tau \frac{k}{N_f N_c}\right), \tag{19}$$

which is the noisy channel impulse response. Assuming that the actual channel impulse response is present only within the GI length while the noise due to the AWGN is uniformly distributed over an entire range, we replace $\hat{h}(\tau)$ with zero for $\tau \geq N_g$ and apply $N_f N_c$-point FFT to obtain the noise-reduced instantaneous channel gain estimate $\{\tilde{H}(k);\ k = 0 \sim N_f N_c - 1\}$ [11]. This is called the delay-time domain windowing technique.

3.1.2 Phase-Rotated Pilot

Letting $t = t' + nN_c$, Eq. (16) can be rewritten as

$$P(k) = \sum_{n=0}^{N_f - 1} \sum_{t'=0}^{N_c - 1} p(t' + nN_c) \exp\left(-j2\pi k \frac{n}{N_f}\right) \times \exp\left(-j2\pi k \frac{t'}{N_f N_c}\right) \tag{20}$$

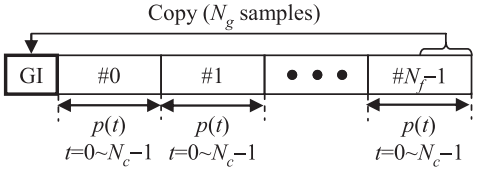

Fig. 5 Repeated pilot.

The $k = iN_f$th frequency component of the pilot frame, whose frequency corresponds to the ith subcarrier of OFDM, can be expressed, using Eq. (14), as

$$P(k = iN_f) = \sum_{n=0}^{N_f - 1} P(i, n). \tag{21}$$

It can be understood from Eq. (21) that the $k = iN_f$th orthogonal frequency component of the pilot frame is the sum of the ith subcarrier components of N_f pilot OFDM symbols in one frame interval. In Sect. 3.1 (1), we assumed that $|P(i, n)| = 1$. When a binary sequence is used as the pilot sequence, $|P(k)|$ at some frequencies may fall to zero. Figure 4 shows the variation of $|P(k)|$ when a PN sequence with a repetition period of 127 is used as the pilot. It is seen from Fig. 4 that some frequency components become zero. This indicates that the channel estimation accuracy is significantly degraded when a binary sequence is used as the pilot. In this paper, to solve this problem, the phase rotation is applied to the pilot OFDM symbol as

$$P_{rot}(i, n) = P(i, n) \exp(jn\theta_p), \tag{22}$$

which is used instead of $P(i, n)$ in Eq. (14). In Fig. 4, $|P(k)|$ using the phase rotation $\theta_p = \pi/2$ rad is plotted. By applying the phase rotation to the pilot sequence, no frequency component becomes zero.

Using MMSE-CE and the delay-time domain windowing technique, the noise-reduced channel gain estimate $\{\tilde{H}(k);\ k = 0 \sim N_f N_c - 1\}$ is obtained.

3.1.3 Repeated Pilot

The same pilot OFDM symbol is repeated N_f times in the pilot frame as shown in Fig. 5. At the receiver, each received pilot OFDM symbol is decomposed by N_c-point FFT into the frequency-domain signal $\{R_p(i, n);\ i = 0 \sim N_c - 1\}$, $n = 0 \sim N_f - 1$. The channel gain estimate $\{\hat{H}(i, n);\ i = 0 \sim N_c - 1\}$, $n = 0 \sim N_f - 1$, can be obtained by removing the pilot modulation [8] as

$$\hat{H}(i, n) = \frac{R_p(i, n) P^*(i, 0)}{|P(i, 0)|^2},\ i = 0 \sim N_c - 1. \tag{23}$$

The instantaneous channel gain estimate $\{\hat{H}(i);\ i = 0 \sim N_c - 1\}$ can be obtained as

$$\hat{H}(i) = \frac{1}{N_f} \sum_{n=0}^{N_f - 1} \hat{H}(i, n), \quad i = 0 \sim N_c - 1. \tag{24}$$

FDE requires the channel gain at the frequency of $k/(N_f N_c T_c)$, $k = 0 \sim N_f N_c - 1$; however the use of the repeated pilot provides the channel gain estimate only at the frequency of $i/(N_c T_c)$, $i = 0 \sim N_c - 1$. Therefore, a frequency-domain interpolation technique is necessary. We apply the delay-time domain windowing technique to reduce the noise while interpolating the initial channel gain estimate $\{\hat{H}(i);\ i = 0 \sim N_c - 1\}$ to obtain the noise-reduced channel gain estimate $\{\tilde{H}(k);\ k = 0 \sim N_f N_c - 1\}$. Below, we derive $\tilde{H}(k)$ which is expressed as an interpolation of the initial channel gain estimate $\{\hat{H}(i); i = 0 \sim N_c - 1\}$. First, the channel impulse response estimate $\{\hat{h}(\tau);\ \tau = 0 \sim N_c - 1\}$ is obtained by applying an N_c-point IFFT to $\{\hat{H}(i);\ i = 0 \sim N_c - 1\}$. Then, $\hat{h}(\tau)$ is extended to the range of $\tau = 0 \sim N_f N_C - 1$. However, since the actual channel impulse response $h(\tau)$ is present only in the range of $\tau = 0 \sim (N_g - 1)$, $\hat{h}(\tau)$ can be replaced by zero in the range of $\tau = N_g \sim N_f N_c - 1$. Finally, by applying an $N_f N_c$-point FFT to $\{\hat{h}(\tau);\ \tau = 0 \sim N_f N_c - 1\}$, the noise-reduced channel gain estimate $\{\tilde{H}(k);\ k = 0 \sim N_f N_c - 1\}$ is obtained as

$$\tilde{H}(k) = \frac{1}{N_f N_c} \sum_{i=0}^{N_c-1} \hat{H}(i) \exp\left\{-j\pi(N_f N_c - 1)\frac{k - iN_f}{N_f N_c}\right\} \times \frac{\sin\{\pi(k - iN_f)\}}{\sin\left(\pi\dfrac{k - iN_f}{N_f N_c}\right)}. \quad (25)$$

It should be noted that the autocorrelation function of the repeated pilot has periodic peaks at every N_c samples and therefore, the repeated pilot cannot be used for the frame synchronization. The frame synchronization can be done by making use of the fact that the same CP waveform (at the end of the frame) appears in the GI (at the beginning of the frame) [13].

3.2 Time-Domain Interpolation

So far, we pointed out the problem of the binary-pilot and then proposed two alternative pilots.

As fading becomes faster, the tracking ability against fading tends to be lost when using only pilot-assisted channel estimation. To improve the tracking ability, the time-domain polynomial interpolation can be introduced in addition to pilot-assisted channel estimation [14]. In this paper, we apply the 1st-order interpolation [15].

We assume that the pilot frame is periodically transmitted, each followed by M data frames. In the 1st-order interpolation, the channel estimate $\{\tilde{H}_m^q(k);\ k = 0 \sim N_f N_c - 1,\ m = 1\text{–}M\}$ at the mth frame between the qth pilot and the $(q+1)$th pilot can be obtained as

$$\tilde{H}_m^q(k) = \frac{M + 1 - m}{M + 1}\tilde{H}_0^q(k) \frac{m}{M + 1}\tilde{H}_0^{q+1}(k), \quad (26)$$

where $\tilde{H}_0^q(k)$ corresponds to the channel estimate at the qth pilot frame.

4. Computer Simulation

4.1 Simulation Condition

Table 1 summarizes the simulation condition. The fading channel is assumed to be a frequency-selective Rayleigh fading channel having a sample-spaced $L = 16$-path exponential power delay profile with decay factor α. One pilot frame is followed by 64 data frames ($M = 64$) as shown in Fig. 6. Binary phase shift keying (BPSK) is used for the pilot modulation. An M-sequence having a 127-bit repetition period is used as the pilot sequence. For comparison, the ideal channel estimation is considered, in which $\{H(k);\ k = 0 \sim (N_f N_c - 1)\}$ for FDE are obtained from Eq. (6) by using the channel impulse response $h(\tau)$ at the first OFDM symbol of each received frame.

In the phase-rotated pilot channel estimation, the accuracy of channel estimation depends on the type of data modulation of the pilot sequence, the frame size N_f, and the phase rotation θ_p. Figure 7 plots the variance of $|P(k)|$ of the phase-rotated pilot as a function of the phase rotation θ_p for the case of BPSK and $N_f = 2$. It is seen from Fig. 7 that $\theta_p = \pi/2$ and $3\pi/2$ provide the lowest amplitude variance. Below, we use $\theta_p = \pi/2$ for the phase-rotated pilot channel estimation.

4.2 Comparison of Pilot Designs

The BER performance of orthogonal MC DS-CDMA with FDE using the pilot-assisted channel estimation (without the time-domain 1st-order interpolation) is plotted in Fig. 8 as a function of the average received E_b/N_0 (=g$0.5SF(E_c/N_0)(1 + 1/M)(1 + N_g/(N_f N_c))$) for a very slow fading environment ($f_D \to 0$) when $SF = C = 4$ (Fig. 8(a))

Table 1 Simulation condition.

Modulation	Data	QPSK, 16QAM
	Pilot	BPSK
Transmitter	No. of subcarriers	N_c=64
	Frame size	N_f=2
	Spreading factor	SF=4, 16
	Spreading code	Walsh-Hadamard
	Code multiplexing order	C=SF
	GI	N_g=16
Channel model	Fading	Frequency-selective Rayleigh fading
	Power delay profile	L=16-path exponential power delay profile
	Decay factor	α=0, 6, ∞ dB
Receiver	FFT/IFFT block size	$N_f N_c$
	FDE	MMSE

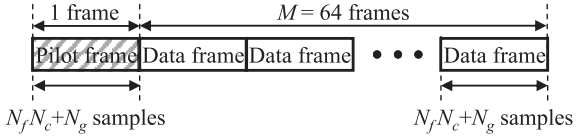

Fig. 6 Transmit frame structure.

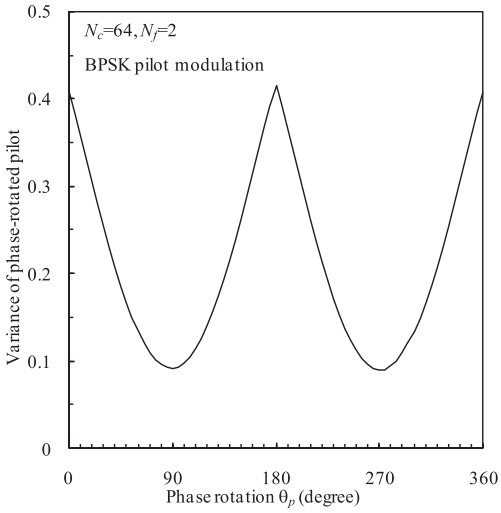

Fig. 7 Amplitude variance of the phase-rotated pilot.

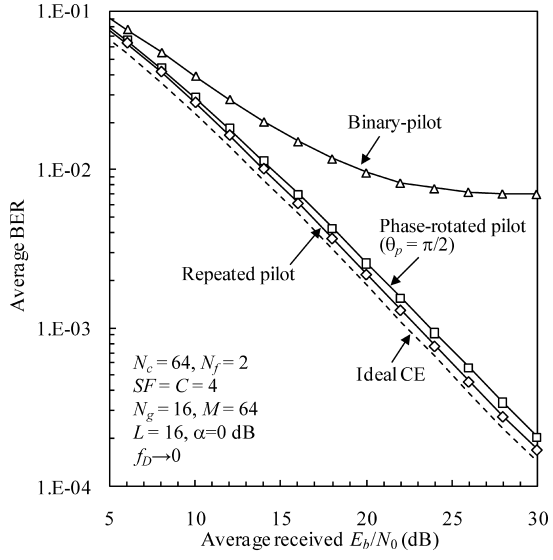

(a) SF=C=4.

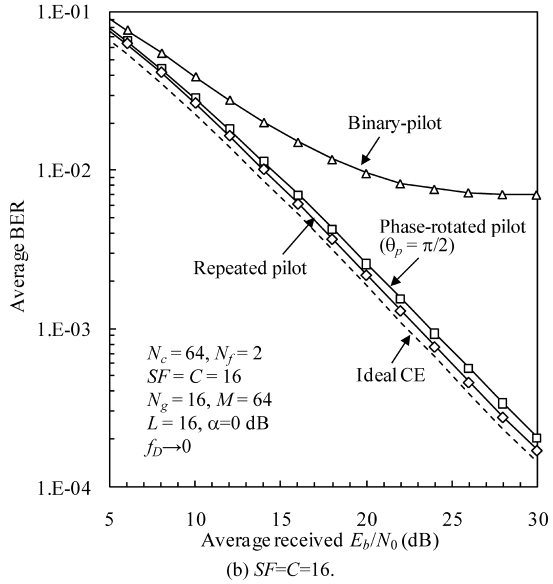

(b) SF=C=16.

Fig. 8 Comparison of pilot designs.

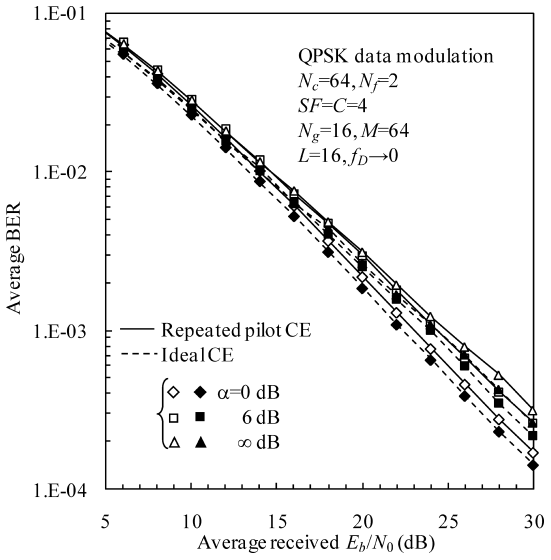

Fig. 9 Impact of decay factor α.

and $SF = C = 16$ (Fig. 8(b)). For comparison, the BER performance with the ideal channel estimation is also plotted. The binary-pilot significantly degrades the BER performance compared to the phase-rotated pilot and the repeated pilot. By applying the phase rotation to the binary-pilot, the BER performance can be significantly improved. However, the phase-rotated pilot is slightly inferior to the repeated pilot. This is because the amplitude $|P(k)|$ of the phase-rotated pilot is not constant over the signal bandwidth even if the optimum phase rotation θ_p is used (see Fig. 4). On the other hand, the repeated pilot has the constant amplitude $|P(k)|$ for all k and therefore, better channel estimation accuracy can be achieved, yielding better BER performance than using the phase-rotated pilot. Both for $SF = C = 4$ and for $SF = C = 16$, the E_b/N_0 degradation for BER = 10^{-3} from the ideal channel estimation is only about 0.6 dB with the channel estimation using the repeated pilot (about 0.07 dB is due to the pilot insertion). Below, the channel estimation using the repeated pilot is only considered.

4.3 Impact of Decay Factor

The impact of the decay factor α on the BER performance using QPSK data modulation is plotted in Fig. 9 for the channel estimation using the repeated pilot when $SF = C = 4$. The BER performance is seen to degrade as α increases (the channel frequency-selectivity gets weaker). This performance degradation is due to the decreasing the frequency diversity gain. However, the E_b/N_0 degradation for BER = 10^{-3} from the ideal CE is only about 0.6 dB irrespective of α.

4.4 Impact of Data Modulation

The BER performances using QPSK data modulation and 16QAM data modulation are compared in Fig. 10 when

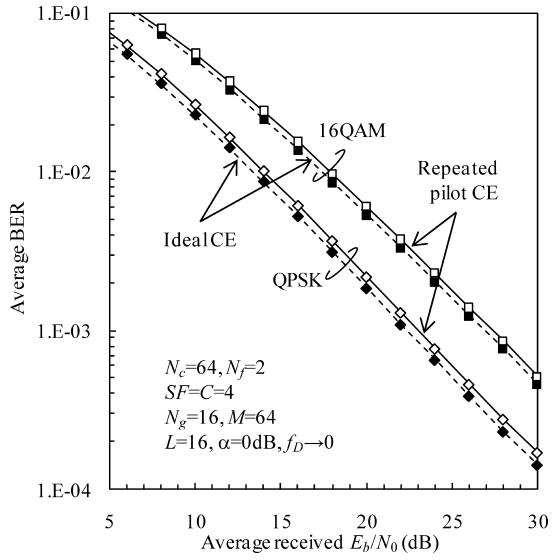

Fig. 10 Impact of data modulation.

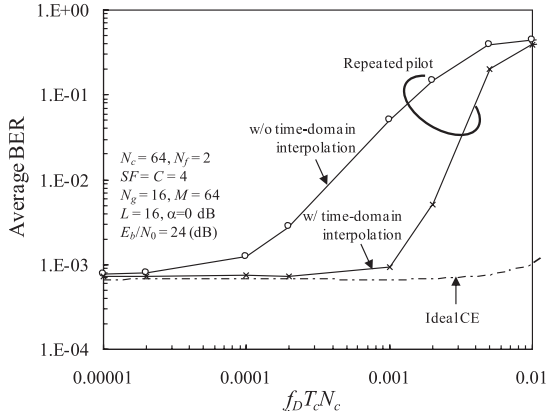

Fig. 11 BER dependency on fading rate.

$SF = C = 4$ and $\alpha = 0$ dB. the E_b/N_0 degradation of 16QAM for BER = 10^{-3} from the ideal CE is almost the same as QPSK.

4.5 Impact of Fading Rate

The BER dependency on the fading rate is plotted as a function of the normalized Doppler frequency $f_D T_c N_c$ for the channel estimation using the repeated pilot in Fig. 11 when the average received $E_b/N_0 = 24$ dB and $SF = C = 4$. The time-domain 1st-order interpolation is used. For comparison, the BER performance with the channel estimation using only the repeated pilot (w/o time-domain interpolation) and that with the ideal channel estimation are also plotted. The tracking ability can be improved by using the time-domain 1st-order interpolation. The use of the repeated pilot and the time-domain 1st-order interpolation can provide almost the same BER value up to $f_D T_c N_c = 0.001$ which corresponds to a terminal moving speed of 340 km/h for 5 GHz carrier frequency and 100 MHz bandwidth. (When $f_D T_c N_c \geq 0.005$, the BER performance for the ideal channel estimation is degraded. This is because the channel gain varies even within one frame and hence, proper FFT cannot be done).

5. Conclusion

In this paper, we proposed a pilot-assisted channel estimation suitable for orthogonal MC DS-CDMA with FDE. The achieved BER performance in a frequency-selective Rayleigh fading channel was evaluated by computer simulation. It was shown that the channel estimation using the repeated pilot gives the good BER performance. The E_b/N_0 degradation for BER = 10^{-3} from the ideal channel estimation in a very slow fading environment ($f_D \to 0$) is only about 0.6 dB (about 0.07 dB is due to the pilot insertion) both for $SF = C = 4$ and for $SF = C = 16$. It was also shown that the use of the repeated pilot and the time-domain 1st-order interpolation can provide almost the same BER value up to $f_D T_c N_c = 0.001$.

References

[1] W.C. Jakes, Jr., ed., Microwave mobile communications, Wiley, New York, 1974.
[2] J.G. Proakis, Digital communications, 2nd ed., McGraw-Hill, 1995.
[3] S. Hara and R. Prasad, "Overview of multicarrier CDMA," IEEE Commun. Mag., vol.35, no.12, pp.126–133, Dec. 1997.
[4] S. Hara and R. Prasad, "Design and performance of multicarrier CDMA system in frequency-selective Rayleigh fading channels," IEEE Trans. Veh. Technol., vol.48, no.5, pp.1584–1595, Sept. 1999.
[5] F. Adachi, D. Garg, S. Takaoka, and K. Takeda, "Broadband CDMA techniques," IEEE Wireless Commun., vol.12, no.2, pp.8–18, April 2005.
[6] S. Kondo and L.B. Milstein, "Performance of multicarrier DS CDMA systems," IEEE Trans. Commun., vol.44, no.2, pp.238–246, Feb. 1996.
[7] K. Tanaka, H. Tomeba, and F. Adachi, "Multi-carrier DS-CDMA transmission with frequency-domain equalization," IEEE WCNC 2007, Hong Kong, March 2007.
[8] K. Takeda and F. Adachi, "Frequency-domain MMSE channel estimation for frequency-domain equalization of DS-CDMA signals," IEICE Trans. Commun., vol.E90-B, no.7, pp.1746–1753, July 2007.
[9] S. Takaoka and F. Adachi, "Pilot-aided adaptive prediction channel estimation in a frequency-nonselective fading channel," IEICE Trans. Commun., vol.E85-B, no.8, pp.1552–1560, Aug. 2002.
[10] Y. (G.) Li, "Pilot-symbol-aided channel estimation for OFDM in wireless systems," IEEE Trans. Veh. Technol., vol.49, no.4, pp.1207–1215, July 2000.
[11] J.J. van de Beek, O. Edfors, M. Sandell, S.K. Wilson, and P.O. Borjesson, "On channel estimation in OFDM systems," Proc. IEEE VTC, pp.815–819, Chicago, IL, July 1995.
[12] D.C. Chu, "Polyphase codes with good periodic correlation properties," IEEE Trans. Inf. Theory, vol.18, no.4, pp.531–532, July 1972.
[13] J.-J. van de Beek, M. Sandell, M. Isaksson, and P.O. Borjesson, "Low-complex frame synchronization in OFDM systems," Proc. IEEE International Conference on Universal Personal Communication (ICUPC'95), pp.982–986, Tokyo, Japan, Nov. 1995.
[14] R. Ku, S. Takaoka, and F. Adachi, "Bit error rate analysis of OFDM with pilot-assisted channel estimation," IEICE Trans. Commun., vol.E90-B, no.7, pp.1725–1733, July 2007.
[15] M. Abramowitz and I.A. Stegun, Handbook of mathematical functions with formulas, fraphs and mathematical tables, 9th printing, Dover, New York, 1970.

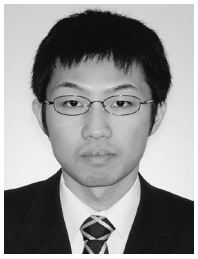

Tomoyuki Shima received his B.S. degree in electronic engineering from Tohoku University, Sendai, Japan, in 2005. Currently he is a graduate student at the Department of Electrical and Communications Engineering, Tohoku University. His research interests include channel estimation for orthogonal MC DS-CDMA.

Hiromichi Tomeba received his B.S., M.S., and Dr. Eng. degrees in communications engineering from Tohoku University, Sendai, Japan, in 2004, 2006, and 2008, respectively. Since 2006, he has been a Japan Society for the Promotion of Science (JSPS) research fellow. Currently he is a JSPS postdoctoral fellow at the Department of Electrical and Communications Engineering, Graduate School of Engineering, Tohoku University. His research interests include frequency-domain equalization and antenna diversity techniques for mobile communication systems. He was a recipient of the IEICE RCS (Radio Communication Systems) Active Research Award in 2004 and 2005.

Fumiyuki Adachi received the B.S. and Dr. Eng. degrees in electrical engineering from Tohoku University, Sendai, Japan, in 1973 and 1984, respectively. In April 1973, he joined the Electrical Communications Laboratories of Nippon Telegraph & Telephone Corporation (now NTT) and conducted various types of research related to digital cellular mobile communications. From July 1992 to December 1999, he was with NTT Mobile Communications Network, Inc. (now NTT DoCoMo, Inc.), where he led a research group on wideband/broadband CDMA wireless access for IMT-2000 and beyond. Since January 2000, he has been with Tohoku University, Sendai, Japan, where he is a Professor of Electrical and Communication Engineering at the Graduate School of Engineering. His research interests are in CDMA wireless access techniques, equalization, transmit/receive antenna diversity, MIMO, adaptive transmission, and channel coding, with particular application to broadband wireless communications systems. From October 1984 to September 1985, he was a United Kingdom SERC Visiting Research Fellow in the Department of Electrical Engineering and Electronics at Liverpool University. He was a co-recipient of the IEICE Transactions best paper of the year award 1996 and again 1998 and also a recipient of Achievement award 2003. He is an IEEE Fellow and was a co-recipient of the IEEE Vehicular Technology Transactions best paper of the year award 1980 and again 1990 and also a recipient of Avant Garde award 2000. He was a recipient of Thomson Scientific Research Front Award 2004.